

Morphological phase transitions of thin fluid films on chemically structured substrates

C. Bauer¹, S. Dietrich¹, and A. O. Parry²

¹*Fachbereich Physik, Bergische Universität Wuppertal, D-42097 Wuppertal, Germany*

²*Department of Mathematics, Imperial College, 180 Queen's Gate, London SW7 2BZ, United Kingdom*

(1. April 1999)

Abstract

Using an interface displacement model derived from a microscopic density functional theory we investigate thin liquidlike wetting layers adsorbed on flat substrates with an embedded chemical heterogeneity forming a stripe. For a wide range of effective interface potentials we find first-order phase transitions as well as continuous changes between lateral interfacial configurations bound to and repelled from the stripe area. We determine phase diagrams and discuss the conditions under which these morphological changes arise.

68.10.-m,82.65.Dp,68.45.Gd

A variety of experimental techniques have emerged which allow one to endow solid surfaces with a rich, well-defined and permanent chemical pattern while keeping the surface flat on a molecular scale (see, *e.g.*, ref. [1]). An important application of these structures is microfluidics [2,3], *i.e.*, the guidance of tiny amounts of adsorbed liquids along these chemical microstructures. This enables one to control the microscopic flow of liquids on designated chemical channels and to facilitate the fabrication of “chemical chips” which may act as microlaboratories for the investigation and processing of rare and valuable liquids [4]. Although these applications involve dynamical processes, as a prerequisite it is important to investigate these systems in thermal equilibrium as a function of the thermodynamic parameters pressure (or, equivalently, chemical potential μ) and temperature T . Some recent studies were concerned with the static behaviour of liquid channels on chemical lanes within the micrometre range (see refs. [5] and [6]). On this scale the morphology of the adsorbed liquid is determined by gross features such as the various surface tensions involved. However, with the rapidly proceeding miniaturisation of microstructures in mind, here we are interested in a much smaller scale within which details of the molecular forces become relevant [7].

The paradigmatic system considered here is a chemically heterogeneous surface which, in top view, exhibits a single stripe. The substrate is flat and composed of two different chemical species such that one of them (denoted by “+”) forms a single slab of width a embedded in the other one (denoted by “−”; see fig. 1(a)). Based on a density functional approach [8] it turns out that the liquid-vapour interface of a thin liquidlike layer in contact with the wall interacts with the wall via an *effective* interface potential $\Lambda(x, l(x))$, where $l(x)$ is the local thickness of the layer at the lateral position x . The substrate potential entering into $\Lambda(x, l(x))$ has been obtained from a pairwise summation over all substrate-fluid particle interactions assuming sharp chemical steps at $x = \pm a/2$. Since the system we consider here is translationally invariant in the y direction, Λ does not depend on y . We take both the substrate-fluid (s) and the fluid-fluid (f) interaction potential to be of Lennard-Jones type: $\phi_{s,f}(r) = 4\epsilon_{s,f}((\sigma_{s,f}/r)^{12} - (\sigma_{s,f}/r)^6)$. We choose the two chemical species such that a flat, semi-infinite, and *homogeneous* substrate composed of each of the species *alone* exhibits an effective interface potential $\Lambda_{\pm}(l)$ as depicted in fig. 1(b). (One may interpret these interface potentials as corresponding to a “hydrophilic” ($\Lambda_{-}(l)$) and a “hydrophobic” ($\Lambda_{+}(l)$) surface even for a nonvolatile liquid.) For our choice of potential parameters the outer part of the substrate undergoes a critical wetting transition at $k_B T_w / \epsilon_f = 1.2$, whereas a homogeneous substrate filled with species corresponding to the stripe part exhibits a first-order wetting transition at $k_B T_w / \epsilon_f \approx 1.102$. For the temperature $k_B T / \epsilon_f = 1.1$ considered throughout the paper both substrate types are only partially wet at bulk liquid-vapour coexistence $\mu = \mu_0$, *i.e.*, $\Delta\mu = \mu_0 - \mu = 0$.

Within a simple interface displacement model, which can be derived systematically from density functional theory (see ref. [8]) the equilibrium contour $l(x)$ of the liquid-vapour interface minimizes the functional

$$\Omega_s[l(x)] = \int_A dx dy \Lambda(x, l(x)) + \sigma_{lg} \int_A dx dy \sqrt{1 + \left(\frac{dl(x)}{dx}\right)^2} \quad (1)$$

with the surface area $A = L_x L_y$ of the substrate surface and $\Lambda(x, l) = \Delta\mu \Delta\rho l + \omega(x, l)$ where, as it turns out, $\omega(x, l) = \sum_{i \geq 2} a_i(x) l^{-i}$ for Lennard-Jones potentials, $\Delta\rho = \rho_l - \rho_g$ is the difference in number densities between the bulk phases, and σ_{lg} is the surface tension

associated with the area of the liquid-vapour interface. Instead of the chemical potential one may use the pressure p of the bulk vapour phase as a thermodynamic control parameter. In this case $\Delta\mu = 0$ corresponds to $p = p_{sat}(T)$ at which the vapour phase is saturated. In a pressure-temperature ensemble one has to replace $\Delta\mu\Delta\rho$ by the pressure difference $\Delta p = p_{sat} - p$. In eq. (1) we have omitted the free energy contributions from the wall-liquid interface at $z = 0$ which are constant with respect to $l(x)$. Subtraction of the surface free energy $\Omega_s(l_-)$ corresponding to the homogeneous outer (“-”) substrate yields the line contribution $L_y\Omega_l[l(x)] = \Omega_s[l(x)] - \Omega_s(l_-)$ to the free energy of the fluid configuration associated with the presence of the chemical stripe. $\Omega_s[l(x)]$ (or equivalently, $\Omega_l[l(x)]$) is minimized numerically with respect to $l(x)$ yielding the equilibrium contour within mean field theory.

Using the interface potential $\Lambda(x, l)$ we find equilibrium interfacial morphologies, pertinent examples of which are shown in fig. 2(a). This figure depicts the interface profiles for varying stripe widths a at a fixed value $\Delta\mu = 0.003\epsilon_f$. Within a wide range of values for a there are two different minimal interfaces, one “bound” to and the other “repelled” from the stripe area.

Figure 2(b) displays the values of the line free energy density Ω_l corresponding to the interface profiles shown in fig. 2(a). For large a the solution bound to the stripe area has a lower line free energy Ω_l than the solution repelled from the stripe. As a is decreased the latter solution is favoured in terms of the free energy. Thus at some value $a = a_t$ there is a phase transition between both interfacial configurations. Due to the break in slope of $\Omega_l(a)$ at $a = a_t$ this transition is first order. We refer to this phenomenon as “morphological phase transition” in the sense that the interface profile $l(x)$ undergoes an abrupt structural change.

The repelled solution exhibits a coverage which is even larger than that corresponding to the homogeneous “-” substrate. This counterintuitive result shows that compared with a homogeneous substrate, one can *increase* the total adsorption by the immersion of a slab of a material that favours *thinner* liquidlike films. The occurrence of this phenomenon persists if the depth of the slab is not macroscopically large as in fig. 1(a) but only molecularly small corresponding to a different material within an imprinted overlayer covering a homogeneous underlying substrate. This example shows that gradual changes in the architecture of chemically microstructured devices can lead to abrupt changes in the morphology of adsorbed liquids. We emphasise that such phase transitions are not only of theoretical interest. Their existence illustrates the care required to avoid the unwanted filling of the nonwet space between liquid channels in such devices.

For $|x| \rightarrow \infty$ the interface profile $l(x)$ asymptotically approaches the equilibrium film thickness l_- corresponding to the outer part of the substrate. If the stripe width is sufficiently large, in the middle of the stripe area $l(x)$ also approaches the equilibrium film thickness l_+ corresponding to the stripe part. In this case, as expected, $l(x)$ smoothly interpolates between the two minima I and II of the interface potentials of the respective homogeneous and flat “+” and “-” substrate taking full advantage of the deep minimum I (see fig. 1(b)). If the stripe width shrinks this gain in free energy decreases accordingly and, moreover, the relative cost for this benefit in terms of the associated increased area of the liquid-vapour interface increases. For $a < a_t$ the loss of free energy by occupying the higher minimum III instead of I is outweighed by the gain in free energy due to a reduced area of the liquid-

vapour interface, leading to the repelled solution because the position of the local minimum III occurs at a larger value of l than for II. The physical nature of this transition is similar to the “unbending” transition on a corrugated wall as described in ref. [9]. As explained in ref. [10] similar effects such as “out-of-phase behaviour” can also occur on nonplanar walls if there are competing minima of the effective interface potential.

For values of $\Delta\mu$ which are larger than a certain critical value $\Delta\mu_c$ the morphological phase transition does not occur, *i.e.*, there is only one stable solution for every value of a . Figure 3 shows the behaviour of the liquid-vapour interfaces for $\Delta\mu = 0.014\epsilon_f > \Delta\mu_c$. In this case the interface profile gradually changes from a repelled configuration for small a to a bound configuration for large a . The corresponding line free energy Ω_l is an analytic function that does not exhibit a cusp singularity and associated metastable branches. Figure 4 displays the line of first-order phase transitions in the $(a, \Delta\mu)$ plane at which the bound and the repelled solutions coexist. Within the present mean field description this line ends at a critical point with $\Delta\mu_c \approx 0.010\epsilon_f$ and $a_c \approx 3.8\sigma_f$.

The number of degrees of freedom involved in the morphological phase transition is proportional to the volume $L_y a (l_- - l_+)$ and thus quasi-onedimensional. Therefore the system cannot support a phase transition in the strict sense of statistical mechanics. Actually the fluctuations are so strong that at the phase boundary shown in fig. 4 the system cannot sustain the sharp coexistence between the bound and the repelled configuration. Instead the system will break up into domains along the y direction with alternating regions of increased and reduced coverage with the positions of the domain boundaries fluctuating. This leads to a rounding of the first-order phase transition due to the aforementioned finite-size effect in two directions and eliminates the critical point shown in fig. 4. However, for large values of a or $l_- - l_+$ the number of degrees of freedom involved becomes quasi-twodimensional so that the rounding of the first-order phase transition sharpens up turning it ultimately into a true discontinuity. Following the general ideas of finite size scaling of first-order phase transitions [11] one can estimate the width $2\delta\mu$ of the rounding around the mean field location $\Delta\mu_t$ of the phase transition according to the implicit equation

$$|\Delta\Omega_l(T, a, \Delta\mu_t(a) + \delta\mu(a))| \lesssim \frac{k_B T}{\xi_b} \exp\left(-\frac{a\Sigma_l(T, \Delta\mu_t(a))}{k_B T}\right) \quad (2)$$

where ξ_b is the bulk correlation length (which is of the order of σ_f) and $\Sigma_l \approx \sigma_{lg}(l_- - l_+)$ estimates the cost in free energy to maintain an interface between two domains as described above; $\Delta\Omega_l$ is the difference in line free energies between the bound and the repelled solution (compare refs. [12] and [13]). A rough numerical estimate of $\delta\mu$ yields the boundaries of the smeared out transition region which are indicated by the dashed lines in fig. 4. Whereas far from the mean field critical point the width of the transition region is exponentially small such that the transition is quasi-first order, for $\Delta\mu$ increasing towards $\Delta\mu_c$ the rounding of the phase transition becomes significant.

In closing we note that the only prerequisite for the occurrence of the morphological phase transition described here is that the effective interface potentials of the materials involved exhibit the gross features shown in fig. 1(b). This holds both for volatile and nonvolatile liquids and does not depend on a particular type of interaction potential or thermodynamic ensemble. Such morphological transitions also occur for other shapes of chemical substrate heterogeneities such as periodic arrays of stripes and circular or even

irregular areas. A variety of experimental techniques such as reflection interference contrast microscopy (RICM) [14] or a force microscope used in tapping mode [15] are being developed which allow one to scan the morphology of fluid films with a spatial resolution down to fractions of a nanometre. The detection of the morphological phase transition predicted here could serve as a promising testing ground for the development of such experimental techniques.

ACKNOWLEDGMENTS

C.B. and S.D. gratefully acknowledge financial support by the German Science Foundation within the Special Research Initiative *Wetting and Structure Formation at Interfaces*.

REFERENCES

- [1] Y. Xia and G.M. Whitesides, *Annu. Rev. Mater. Sci.* **28**, 153 (1998); D. W. L. Tolfree, *Rep. Prog. Phys.* **61**, 313 (1998); F. Burmeister, C. Schäfle, B. Keilhofer, C. Bechinger, J. Boneberg, and P. Leiderer, *Adv. Mater.* **10**, 495 (1998).
- [2] J. B. Knight, A. Vishwanath, J. P. Brody, and R. H. Austin, *Phys. Rev. Lett.* **80**, 3863 (1998).
- [3] M. Grunze, *Science* **283**, 41 (1999); and references therein.
- [4] R. F. Service, *Science* **282**, 399 (1998).
- [5] P. Lenz and R. Lipowsky, *Phys. Rev. Lett.* **80**, 1920 (1998).
- [6] H. Gau, S. Herminghaus, P. Lenz, and R. Lipowsky, *Science* **283**, 46 (1999).
- [7] S. Dietrich, *Fluids in contact with structured substrates*, proceedings of the NATO-ASI on *New approaches to old and new problems in liquid state theory: inhomogeneities and phase separation in simple, complex, and quantum fluids*, held at Patti Marina, Italy, July 7-17, 1998, edited by C. Caccamo (Kluwer, Dordrecht, in press).
- [8] C. Bauer and S. Dietrich, preprint cond-mat/9812266 (1998); *Eur. Phys. J. B*, in press (1999); and references therein.
- [9] C. Rascón, A. O. Parry, and A. Sartori, preprint cond-mat/9902070 (1999); *Phys. Rev. E*, in press (1999).
- [10] C. Rascón and A. O. Parry, *Phys. Rev. Lett.* **81**, 1267 (1998).
- [11] V. Privman and M. E. Fisher, *J. Stat. Phys.* **33**, 385 (1983); *J. Appl. Phys.* **57**, 3327 (1985).
- [12] M. P. Gelfand and R. Lipowsky, *Phys. Rev. B* **36**, 8725 (1987).
- [13] T. Bieker and S. Dietrich, *Physica A* **252**, 85 (1998); **259**, 466 (1998).
- [14] G. Wiegand, T. Jaworek, G. Wegner, and E. Sackmann, *J. Colloid Interface Sci.* **196**, 299 (1997).
- [15] S. Herminghaus, A. Fery, and D. Reim, *Ultramicroscopy* **69**, 211 (1997); T. Pompe, A. Fery, and S. Herminghaus, *Langmuir* **14**, 2585 (1998).

FIGURES

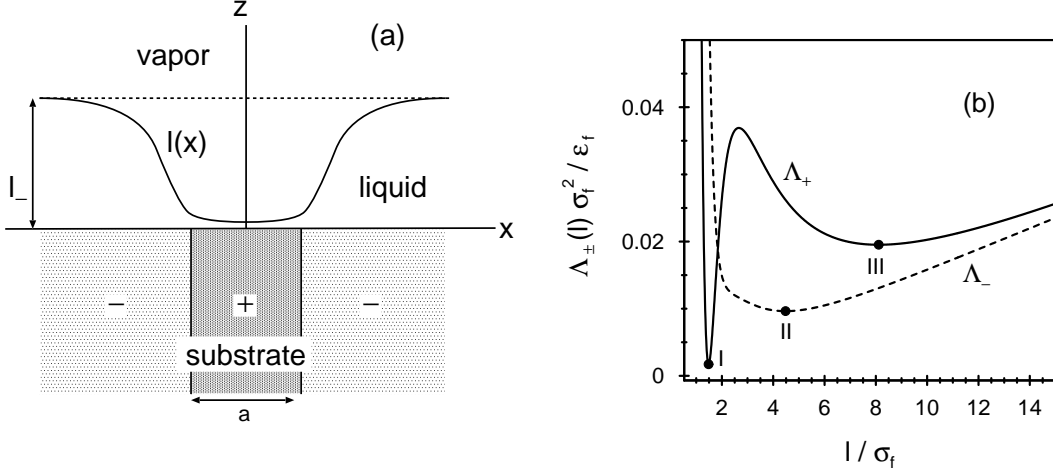


FIG. 1. (a) Cross section of the morphology of a liquidlike wetting film covering a planar substrate that contains a slab of different material. The substrate surface is located at $z = 0$ and the system is translationally invariant in the y direction. Viewed from the top the stripe region is filled with chemical species denoted by “+” and extends from $x = -a/2$ to $x = a/2$, *i.e.*, the stripe width is a . $l_- = l(|x| \rightarrow \infty)$ is the equilibrium thickness of the liquidlike wetting film corresponding to a flat, homogeneous substrate composed of “-” particles alone. The stripe and the outer region favour a thin and a thick wetting layer, respectively. (b) The effective interface potentials $\Lambda_+(l)$ (full line) and $\Lambda_-(l)$ (dashed line) of the flat and *homogeneous* substrates composed of the chemical species “+” and “-”, respectively, are minimized for $l = l_+$ and $l = l_-$, respectively. These interface potentials correspond to $k_B T / \epsilon_f = 1.1$ and $\Delta\mu / \epsilon_f = 0.003$ (as, c.f., in fig. 2). For $\Delta\mu \rightarrow 0$ the positions of the minima II and III are shifted towards larger values of l and to $l = \infty$, respectively, whereas I remains basically unchanged. The global minima I and II of $\Lambda_{\pm}(l)$ correspond to the equilibrium film thickness of the liquidlike film adsorbed on the respective *homogeneous* substrate. $\Lambda_{\pm}(l \rightarrow \infty)$ increases linearly as $\Delta\mu \Delta\rho l$. $\Lambda_{\pm}(\Delta\mu = 0, l = \infty) = 0$ and $\Lambda_{\pm}(\Delta\mu = 0, l = l_{I,II}) < 0$, *i.e.*, at two-phase coexistence $\Delta\mu = 0$ and at the above temperature both types of substrates are only partially wet.

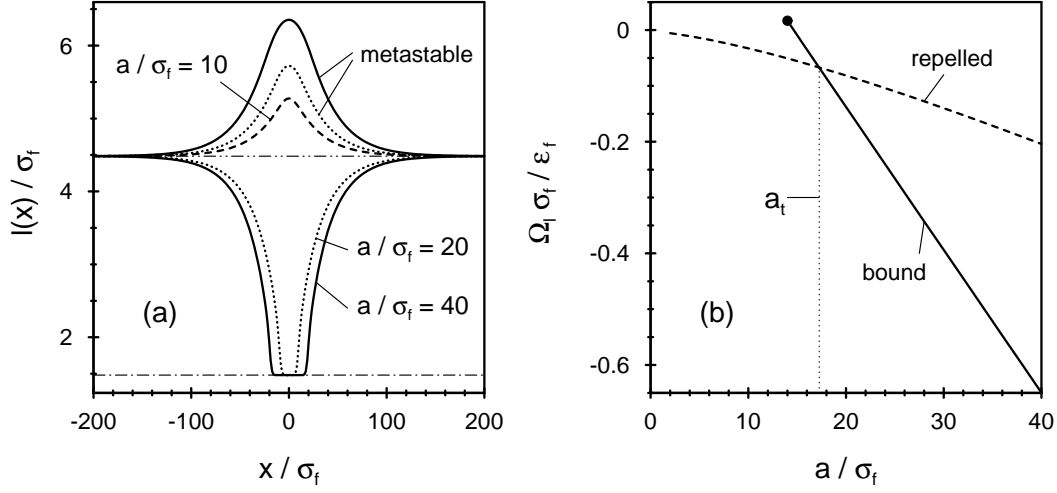


FIG. 2. (a) Liquid-vapour interfaces on the stripe-shaped heterogeneity calculated for $k_B T / \epsilon_f = 1.1$ and $\Delta \mu / \epsilon_f = 3 \cdot 10^{-3}$ based on the effective interface potentials shown in fig. 1(b). The interface profiles are calculated for $a / \sigma_f = 10$ (dashed line), 20 (dotted lines), and 40 (full lines). For $a = 10 \sigma_f$ there is only a repelled solution. The dash-dotted lines indicate the equilibrium film thicknesses l_+ ($-\cdot$) and l_- ($-\cdot\cdot$). (b) That part of the line contribution Ω_l to the grand canonical potential which depends functionally on $l(x)$, for the same choice of parameters as in (a). At $a = a_t \approx 17.4 \sigma_f$ there is a first-order phase transition from the repelled (dashed line) to the bound solution (full line). The dot indicates the end of the metastable branch of bound solutions for $a < a_t$. The metastable branch of repelled solutions extends far to large values of a .

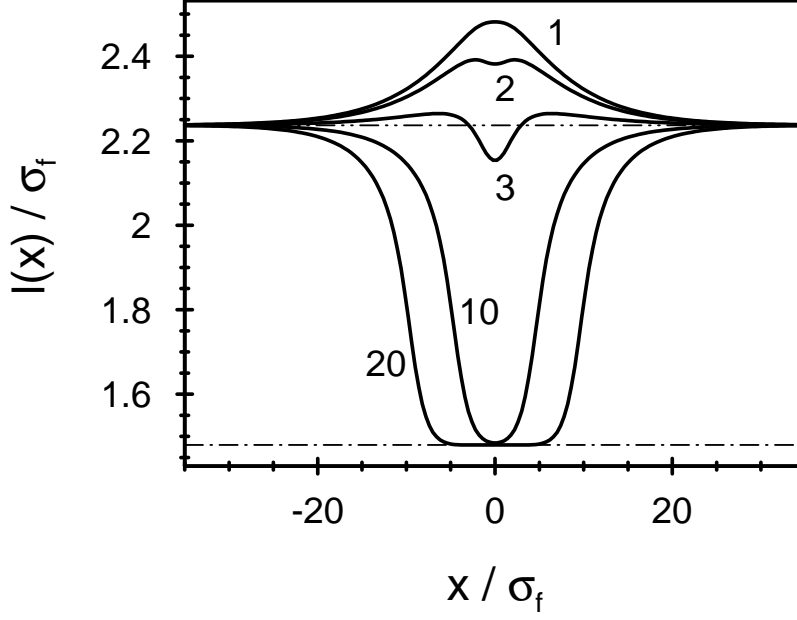


FIG. 3. Profiles of the liquid-vapour interface exposed to substrates as shown in fig. 1(a) for $k_B T / \epsilon_f = 1.1$ and $\Delta\mu = 0.014\epsilon_f > \Delta\mu_c$. The numbers accompanying each graph indicate the corresponding value of the stripe width a in units of σ_f . The same set of interaction parameters is used as for fig. 2. The dash-dotted lines indicate the equilibrium film thicknesses l_+ ($-\cdot$) and l_- ($-\cdot\cdot$) (see fig. 1(b)). Since the system is above the critical point $(\Delta\mu_c, a_c)$ of the morphological phase transition there is only one stable solution for every value of a . There is no first-order phase transition and $\Omega_l(a)$ is a smooth function.

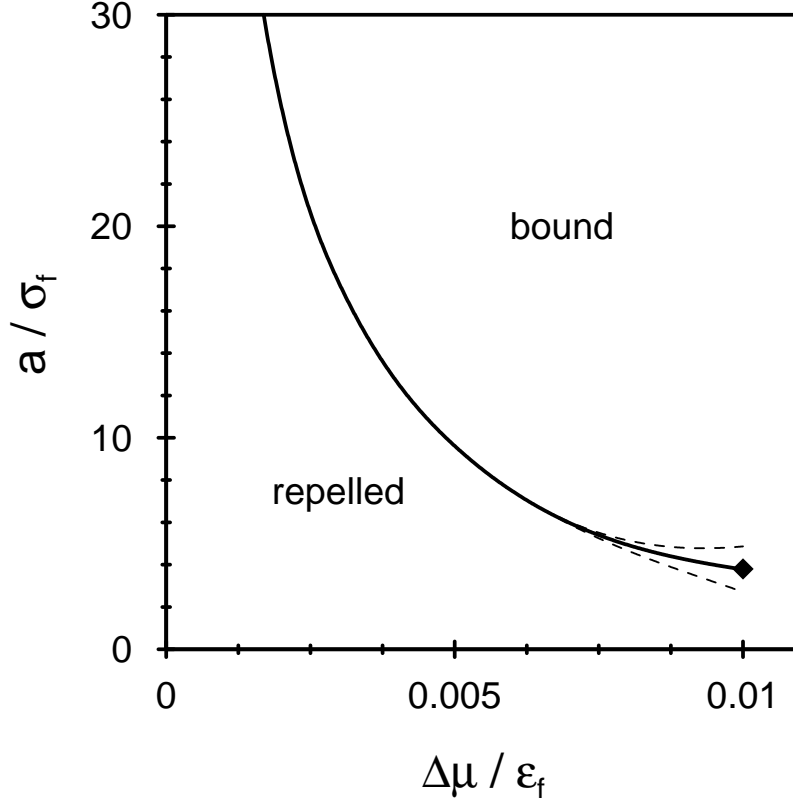


FIG. 4. Line of first-order phase transitions between solutions bound to and repelled from the stripe area (full line). The same set of interaction parameters is used as for figs. 2 and 3. Within mean field theory the line ends at a critical point which is indicated by the diamond symbol. For decreasing $\Delta\mu$ the line of phase coexistence extends further up to higher values of a . The dashed lines indicate the region within which the rounding of the first-order transition due to thermal fluctuations takes place. For decreasing values of a , *i.e.*, upon approaching the mean field critical point, this rounding becomes more and more important. Thus the fluctuations erase the phase transition near a_c and eliminate the associated critical point. For large values of a the fluctuation-induced rounding of the first-order phase transition is practically not detectable.